ISSN: 2414-1895 DOI: 10.6919/ICJE.202203_8(3).0011

Trajectory Prediction of Buoy Drift based on Improved Complex Valued Neural Network

Liangkun Xu[1,2]

[1] Merchant Marine College, Shanghai Maritime University, Shanghai 201306, China

[2] Navigation College, Jimei University, Xiamen 361021, Fujian, China

Abstract

This paper presents a buoy drift trajectory prediction algorithm based on improved complex valued neural network. Taking the longitude of the buoy as the real part of the input and the latitude as the imaginary part of the input, the complex input of the complex valued neural network is constructed. All longitudes and latitudes on the earth are perpendicular to each other. This satisfies that the real and imaginary parts of the complex form an orthogonal unit basis. The drift trajectories of buoys with different reporting intervals are estimated. The algorithm is tested by using the position data of buoys 11a and 2 in Meizhou Bay, Fujian Province. The effects of reporting interval, drift distance, adaptive factor and noise covariance on the estimated longitude are analyzed and compared. Experimental results and error analysis show that the new algorithm is superior to other algorithms in trajectory prediction. The longitude error and latitude error of the new method are 3.21e-04 and 6.36e-05 respectively, which is lower than the original algorithm. Therefore, this algorithm can be used to accurately predict the drift trajectory of dynamic time interval buoy.

Keywords

Neural Network; Buoy Drift; Trajectory Prediction.

1. Introduction

Buoys are artificial markers used to mark obstructions and channel boundaries, instructing ships to navigate and avoid obstacles. However, buoys are easy to drift due to the influence of wind, current, waves and ship's traveling waves, thus affecting the navigation safety of ships.

For this issue, Gan et al. proposed a method for early warning of beacon drift based on Kalman filter and Iterative Self-Organizing Data Analysis Technique (ISODATA) [1]. Xu proposed research on navigation mark drift early warning and cloud management platform [2]. Cheng demonstrated and proposed an optimal calculation method for the length of the beacon anchor chain based on the water level information at the time of marking [3]. Zhou et al. proposed a method for calculating the drift characteristics of inland navigation aids based on Kalman filter and K-means++ algorithm [4]. Chen used the product season model to predict the position of the light buoy in the deep-water channel of the Yangtze Estuary, and verified the effect of displacement early warning [5]. Zhou et al. used Person correlation analysis method and regression analysis method to construct a navigation mark drift model under the action of tidal current field [6]. Wu et al. established a mathematical model for buoy excursion prediction using the product season model, and tested the accuracy of the prediction results based on the telemetry data of the No.1 light buoy in Meizhou Bay [7].

In recent years, Complex-valued neural network (CVNN) has received extensive attention from the academic community for its strong mapping ability and good adaptability. CVNN have been applied in fields where the input data has the ability to interpret naturally in complex domains, especially in

ISSN: 2414-1895 DOI: 10.6919/ICJE.202203_8(3).0011

the field of signal processing. The use of complex numbers enables neural networks to deal with noise on complex planes. Different strategies can be used to transfer many activation functions from the real to the complex domain. Chen studied event-triggered CVNN master-slave synchronization [8]. Song discusses the input state exponential stability of stochastic CVNN with neutral and discrete delays [9]. Huang studied the finite-time passivity and finite-time synchronization of two classes of coupled memristor CVNN with and without time-varying delays [10]. Li uses a deep CVNN trained with AC frequency-phase-amplitude coupled features to separate different regions [11]. Song discusses the synchronization problem of fractional-order CVNNs with reaction-diffusion terms in finite time intervals [12]. Aouiti considers finite-time and fixed-time synchronization problems for time-delay recursive CVNN with discontinuous activation functions and sliding mode control with different parameters [13].

Due to communication congestion and network delays between the coast station and the beacon, sometimes correct position data may not be received, or the position report may not be updated in time. As a result, buoy position update reports typically use different reporting intervals. In order to compensate for the problem that the position data is not updated in time or the estimation error is large, this paper uses an improved complex-valued neural network to estimate the drift of the buoy with different reporting intervals, so that the drift estimation problem of the dynamic interval of the buoy position reporting in the actual situation can be more accurately solved.

2. The Main Factors Affecting the Position of Buoy

The buoy provides navigation assistance services for the safe and convenient navigation of the ship. The position of the buoy has a great impact on the safety of navigation. If the buoy deviates from the position announced by the navigation security department, it will affect the positioning accuracy of the ship, which may cause the ship to deviate.

2.1 Buoy Mooring System

According to experience, the length of the buoy anchor chain will be configured in consideration of the water flow near its location. Generally speaking, the waters with a flow rate below 2kn can be configured according to 3 times the water depth, and those above 2kn can be configured according to 4 times the water depth.

The buoy mooring system is mainly composed of four parts: ground chain, swing chain, suspension chain and tail chain. Figure 1 below is a schematic diagram of the buoy mooring system.

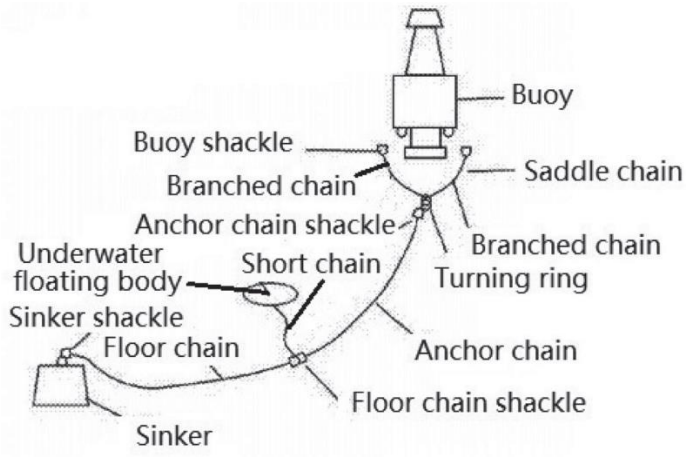

Figure 1. Schematic diagram of buoy mooring system

2.2 Position of the Buoy

The position of the buoy can be divided into the sinking position, the design position and the floating position according to the different definitions.

ISSN: 2414-1895 DOI: 10.6919/ICJE.202203_8(3).0011

(1) The sinking position. When the sinking is fast, the buoy ship is affected by factors such as wind, current, and GPS errors, and there is a certain error between the actual position of the sinking and the theoretical placement position.

(2) The design position. It is the position of the buoy released by the maritime security department, and is generally the theoretical position where the buoy sinks are dropped.

(3) The floating position. It is the position of the floating body of the buoy as seen by the ship, which is the actual position of the floating body under the influence of wind, current and other factors. The floating position changes constantly with external interference. Since the buoy telemetry and remote-control GPS receiver is installed on the floating body, the position data of the buoy collected by the telemetry and remote-control system is the real-time floating position data of the buoy.

2.3 Factors Affecting Buoy Position

2.3.1 Placement Error

When dropping or resetting the buoy, the buoy ship is generally used for operation, and the positioning is based on the drop position of the sunken rock. The launching operation of buoys is a very systematic work. The factors to be considered include hydrometeorology, ship operation, etc. At the same time, it is also necessary to obtain the latest navigation warnings, weather warnings and other information in time.

At the same time, when the sunken stone falls into the water from the side to the seabed, it will advance a certain distance with the speed of the ship, and after the sunken stone falls into the water, it will also slightly deviate from the falling position due to the action of the current.

2.3.2 Buoy Turning Radius

Ideally, the radius of gyration of the buoy $R = \sqrt{L^2 - H^2}$ (as shown in Figure 2), where R is the maximum radius of gyration, L is the length of the anchor chain, and H is the water depth. In fact, the radius of gyration is related to the length of the buoy anchor chain and the water depth. Generally speaking, the actual radius of gyration of the buoy is about 0.8R.

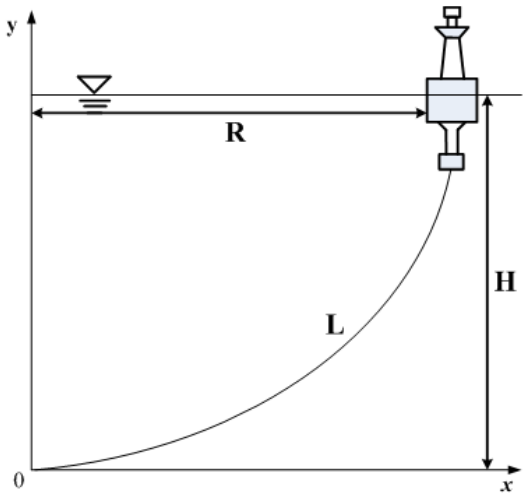

Figure 2. Schematic diagram of buoy turning radius

2.3.3 The Influence of Wind, Waves and Current

The ship is affected by wind, waves and currents, and will drift under the action of wind, waves and currents, and the degree of drift is mainly closely related to the forces of wind, waves and currents[14].

The buoy is affected by wind, waves and currents on the water, and its drift direction depends on the magnitude and direction of the resultant force of these three forces.

ISSN: 2414-1895 DOI: 10.6919/ICJE.202203_8(3).0011

2.3.4 Influence of Ship Traveling Waves

If the speed of the ship in the channel is fast, the ship's traveling wave will be more violent, and the ship's traveling wave will cause the buoy to sway. The size of the ship traveling waves generated by ships of different types, speeds, and tonnages is also different, and relevant researchers have also done some theoretical calculations [15][16].

Due to the high density of navigable ships in Meizhou Bay, various ship types and different ship speeds, it is difficult to calculate the influence of ship traveling waves on buoys using theoretical values.

2.4 Problems Existing in Theoretical Calculation of Buoy Drift Law

From the above analysis of the factors affecting the position of the buoy, it can be seen that the movement of the buoy in the water is the result of a variety of external forces, including natural conditions (wind, current, waves), external factors (ship waves), and human factors (artificial setting), equipment factors (GPS error), floating body attitude (floating body tilt angle), etc. These factors that affect the position of the buoy are all uncertain.

(1)Natural factors: Although the magnitude and direction of wind, current, and waves can be observed, these influencing factors are always changing, not a fixed value.

(2) External factors: Different types of ships and ships with different ship speeds generate different ship traveling waves during navigation. Therefore, the force on the buoy is also different, and the ship flow rate is large, and the arrival of ships is irregular. Therefore, the influence of the ship's traveling wave on the position of the buoy cannot be obtained by accurate calculation.

(3) Human factors: The influence of human factors on the position of the buoy is mainly manifested in the difference in position control when the buoy is set, and the judgment of the supervisor of different staff will affect the position of the sinking block, thereby affecting the position accuracy of the buoy.

(4) Equipment factor: It is mainly GPS error, which is affected by factors such as weather conditions, receiver clock error, etc., and also affects the position accuracy of the buoy, and the error value cannot be obtained through theoretical calculation.

(5) Float inclination angle: The floating body is affected by the wind current, and the attitude will change with it, so that the antenna position deviates from the center of the floating body. At this time, the value measured by the GPS receiver will deviate from the actual center. Due to the uncertainty of wind and current, the inclination angle of the floating body is also changing at any time, and the resulting position error is also difficult to obtain.

It can be seen from the above analysis that the buoy reciprocates and periodically moves around the sinking stone under the action of external force. Since the external force is basically changing at any time, it is difficult to accurately predict the movement law of the floating body through mathematical models.

3. Buoy Drift Dynamic Equation

Device reception delays and communication delays affect the reporting interval for buoy positions. $T(k)$ Defined as the time interval in the buoy position update report, $\varphi(k)$ Indicates the latitude of the buoy, $\lambda(k)$ Indicates the longitude of the buoy, $v(k)$ Indicates the drift speed of the buoy , $\theta(k)$ Indicates the drift direction angle of the buoy. The latitude and longitude of the buoy can be calculated as follows:

$$\varphi(k+1) = \varphi(k) + v(k)T(k)\cos(\theta(k)) \tag{1}$$

$$\lambda(k+1) = \lambda(k) + v(k)T(k)\sin(\theta(k)) \tag{2}$$

ISSN: 2414-1895 DOI: 10.6919/ICJE.202203_8(3).0011

Defined x as the state vector:

$$x(k) = \begin{bmatrix} \varphi(k) \\ \lambda(k) \end{bmatrix} \tag{3}$$

Define $u(k)$ as the control input, Calculated as follows:

$$u(k) = \begin{bmatrix} v(k)T(k)\cos(\theta(k)) \\ v(k)T(k)\sin(\theta(k)) \end{bmatrix} \tag{4}$$

Consider the presence of noise in real systems. Defined w as system noise. The system state equations of equations (1) and (2) can be written as:

$$x(k+1) = x(k) + T(k)u(k) + w(k) \tag{5}$$

Defined z as the measurement vector, ε as measurement noise, The system observation equation can be written as:

$$z(k+1) = x(k+1) + \varepsilon(k+1) \tag{6}$$

4. Trajectory Prediction of Buoy Drift based on Improved CVNN

4.1 CVNN

In complex valued neural network, the input is a complex number z:

$$z = z_R + iz_I \tag{7}$$

$$\varphi = [\varphi_1, \varphi_2, \cdots, \varphi_P] \tag{8}$$

where zR is the real part of the input vector, zI is the imaginary part of z, $\|x\|$ is the Euclidean norm, φ Represents the activation function of the neuron, H is the number of hidden nodes, w is the weight connecting the hidden layer and the output layer, N Indicates the number of input nodes, wR is the real part of w. wI is the imaginary part of w, o represents the output of the neural network:

$$o = W(n)\varphi(z(n)) \tag{9}$$

$$W(n) = [w_1(n), w_2(n), \cdots, w_H(n)] \tag{10}$$

$$w(n) = w_R(n) + w_I(n) \tag{11}$$

The complex valued neural network framework is shown in Figure 3:

ISSN: 2414-1895 DOI: 10.6919/ICJE.202203_8(3).0011

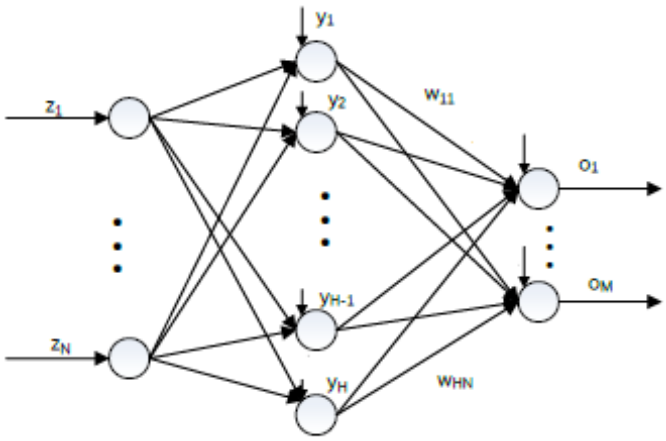

Figure 3. CVNN frame

4.2 Fractional Calculus

Define t as the end point of the integration. Indicates that t0 is the starting point of the integration. For a function x defined in[t0, t], Fractional integral is defined as:

$$ {}_{t_0}D_t^{\alpha}x(t)=\frac{1}{\Gamma(\alpha)}\int_{t_0}^{t}(t-\tau)^{\alpha-1}x(\tau)d\tau \tag{12}$$

where α is the fractional order, τ is the integral variable, Γ is the gamma function:

$$ \Gamma(x)=\int_0^{\infty}e^{-\tau}\tau^{x-1}d\tau \tag{13}$$

Fractional differentiation is defined as:

$$ {}_{t_0}D_t^{\alpha}x(t)=\frac{d^m}{dt^n}\left[\frac{1}{\Gamma(m-\alpha)}\int_{t_0}^{t}(t-\tau)^{m-\alpha-1}x(\tau)d\tau\right] \tag{14}$$

where $\alpha\in[m-1,m)$. m is a positive integer close to α.

4.3 Improved Complex Valued Neural Network

Define d as the expected output. dR is the real part of d, dI is the imaginary part of d. The squared error function is defined as:

$$ E=\frac{1}{2}\sum_{n=1}^{H}[(w\varphi_R(n)-d_R)^2+(w\varphi_I(n)-d_I)^2] \tag{15}$$

$$ d=d_R+d_I \tag{16}$$

note:

$$ g_R=\frac{1}{2}(w\varphi_R-d_R)^2 \tag{17}$$

ISSN: 2414-1895 DOI: 10.6919/ICJE.202203_8(3).0011

$$g_I = \frac{1}{2}(w\varphi_I - d_I)^2 \tag{18}$$

Taking the derivative of (17), we can get:

$$g'_R = y'(w\varphi_R - d_R) \tag{19}$$

Taking the derivative of (18), we can get:

$$g'_I = y'(w\varphi_I - d_I) \tag{20}$$

Taking the second derivative of (17), we can get:

$$g''_R = y''(w\varphi_R - d_R) + (y')^2 \tag{21}$$

Taking the second derivative of (18), we can get:

$$g''_I = y''(w\varphi_I - d_I) + (y')^2 \tag{22}$$

By adjusting the weights, the loss function can be minimized. Note the adjustment increment of wR is Δw_R^n. Note the adjustment increment of wI is Δw_I^n:

$$\Delta w_R^n = w_R^{n+1} - w_R^n \tag{23}$$

$$\Delta w_I^n = w_I^{n+1} - w_I^n \tag{24}$$

$$\Delta w^n = \Delta w_R^n + i\Delta w_I^n \tag{25}$$

Update the rule to:

$$\Delta w_R^n = -\lambda D_{w_R}^{\alpha} E \tag{26}$$

$$\Delta w_I^n = -\lambda D_{w_I}^{\alpha} E \tag{27}$$

Where $\lambda > 0$.

Differentiating E with respect to wR gives:

$$D_{w_R}^{\alpha} E = g'_R \varphi_R \frac{w_R^{1-\alpha}}{\Gamma(2-\alpha)} \tag{28}$$

Differentiating E with respect to wI gives:

ISSN: 2414-1895 DOI: 10.6919/ICJE.202203_8(3).0011

$$D_{w_I}^{\alpha} E = g'_I \varphi_I \frac{w_I^{1-\alpha}}{\Gamma(2-\alpha)} \tag{29}$$

Substitute (28) into (26) to get:

$$\Delta w_R^n = -\lambda g'_R \varphi_R \frac{w_R^{1-\alpha}}{\Gamma(2-\alpha)} \tag{30}$$

Substitute (29) into (27) to get:

$$\Delta w_I^n = -\lambda g'_I \varphi_I \frac{w_I^{1-\alpha}}{\Gamma(2-\alpha)} \tag{31}$$

5. Experiment and Analysis

5.1 Introduction of Experimental Data

The performance of the algorithm is tested with the data of buoy No.11A and No.2 in Meizhou Bay. Taking buoy No. 11A as an example, Table 1 lists the position records of this buoy in 2020.

Table 1. Location of 11A buoy in Meizhou Bay on June 29, 2020

longitude	latitude	time
119.05166667	25.037733333	2020/06/29 04:06
119.05165000	25.037800000	2020/06/29 04:06
119.05168333	25.037716667	2020/06/29 05:06
119.05166667	25.037783333	2020/06/29 05:06
119.05171667	25.037766667	2020/06/29 06:06
119.05175000	25.037550000	2020/06/29 06:06
119.05175000	25.037666667	2020/06/29 07:06
119.05178333	25.037450000	2020/06/29 07:06
119.05180000	25.037500000	2020/06/29 08:06
119.05188333	25.037383333	2020/06/29 08:06
119.05186667	25.037383333	2020/06/29 09:06

The algorithm parameters are set as follows:The initial covariance matrix of the observation noise is $\begin{bmatrix} 0.001 & 0 \\ 0 & 0.001 \end{bmatrix}$.The initial covariance matrix of the state orbit noise is $\begin{bmatrix} 1 & 0 \\ 0 & 1 \end{bmatrix}$.The adaptive factor $\beta = 0.001$.

5.2 Filtering Results for Different Drift Distances

The trajectory of No. 11A buoy using this algorithm for state estimation is shown in Figure 4. The buoy has a long drift distance.

ISSN: 2414-1895 DOI: 10.6919/ICJE.202203_8(3).0011

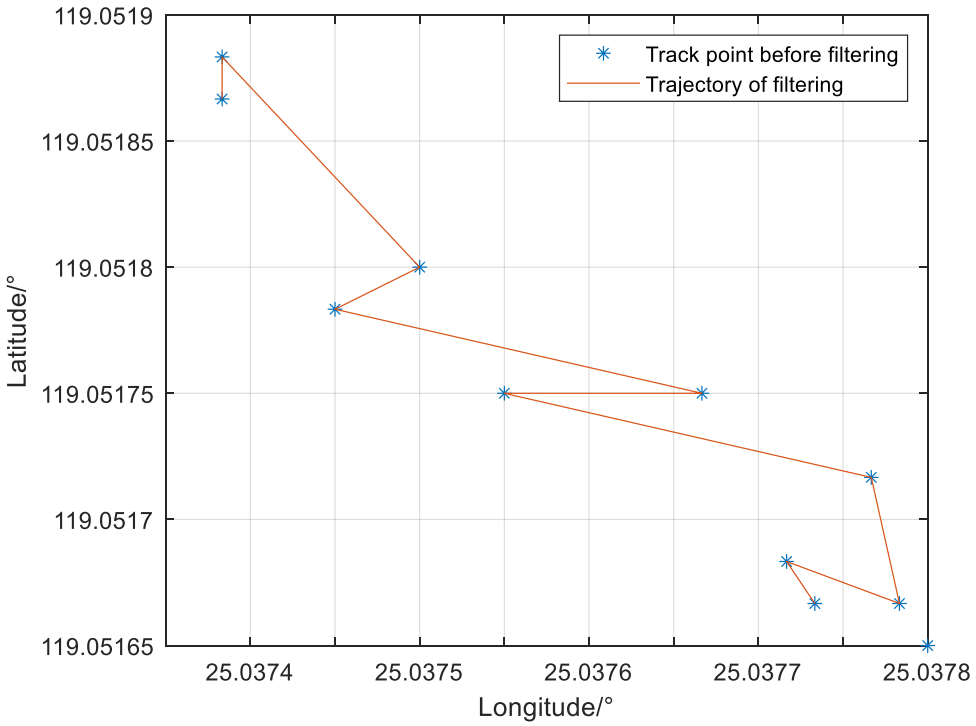

Figure 4. Trajectory prediction of 11A buoy in June 2020

The longitude prediction error is shown in Figure 5.

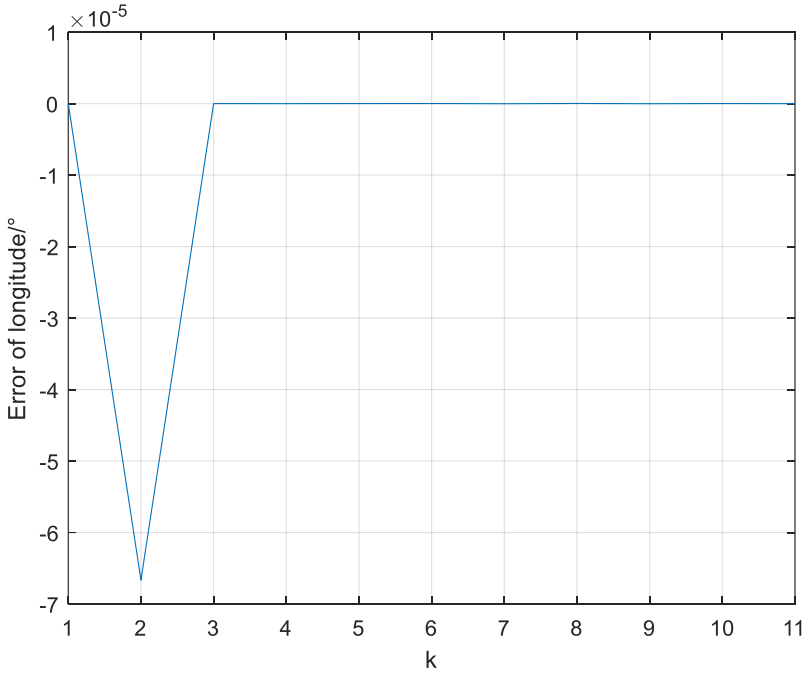

Figure 5. Estimation error of longitude of 11A buoy in June 2020

The latitude prediction error is shown in Figure 6.

ISSN: 2414-1895 DOI: 10.6919/ICJE.202203_8(3).0011

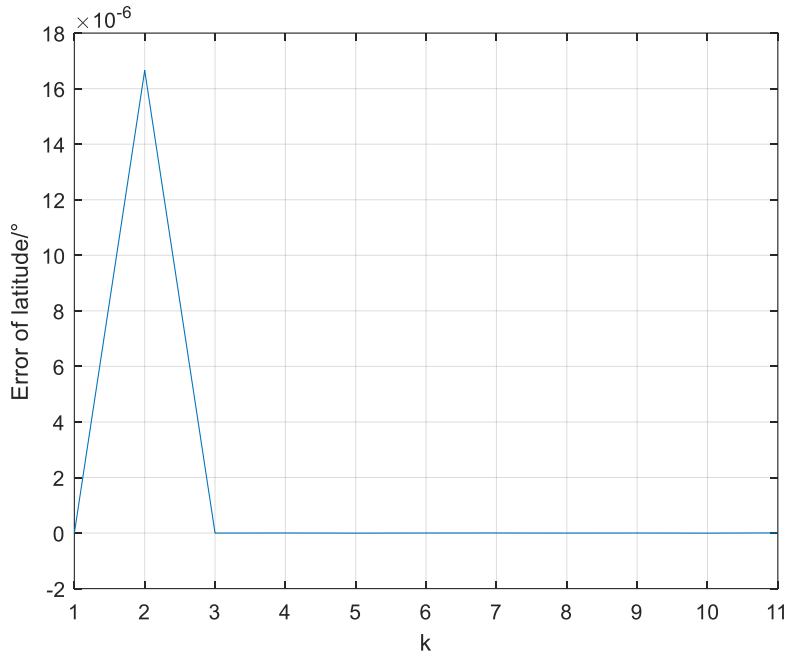

Figure 6. Estimation error of latitude of 11A buoy in June 2020

The trajectory of No.2 buoy using this algorithm for state estimation is shown in Figure 7. The buoy has a short drift distance.

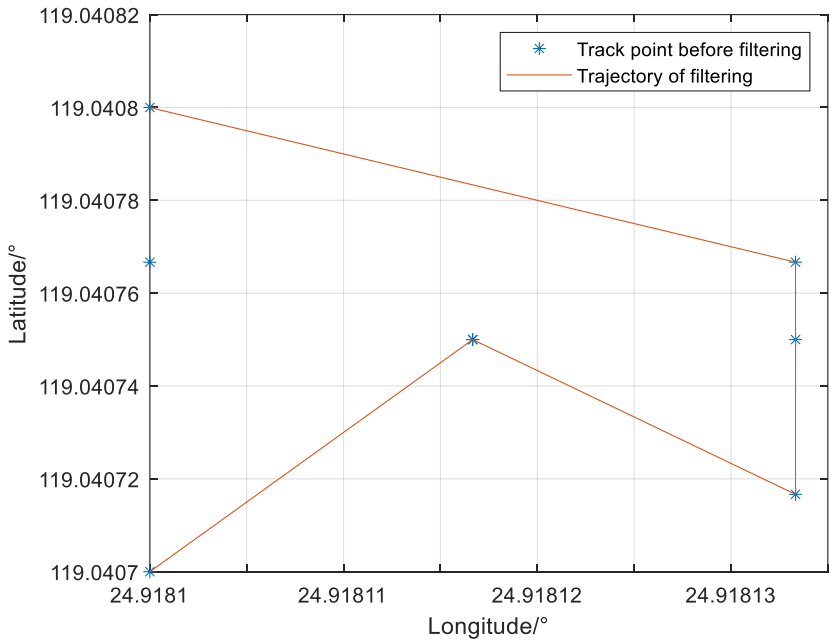

Figure 7. Trajectory prediction of No.2 buoy in June 2020

The longitude prediction error is shown in Figure 8.

ISSN: 2414-1895 DOI: 10.6919/ICJE.202203_8(3).0011

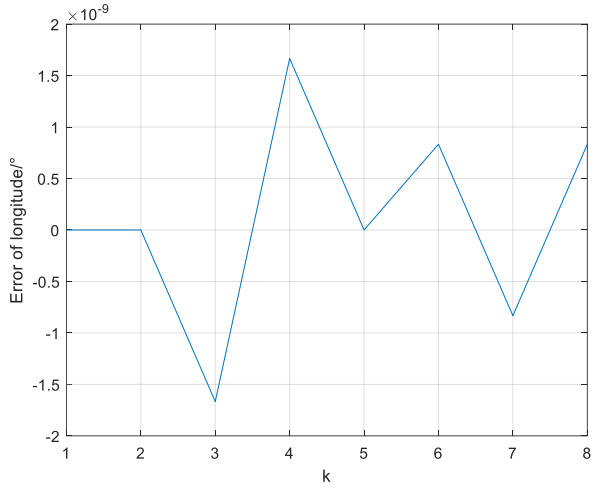

Figure 8. Estimation error of longitude of No.2 buoy in June 2020

The latitude estimation error is shown in Fig. 9.

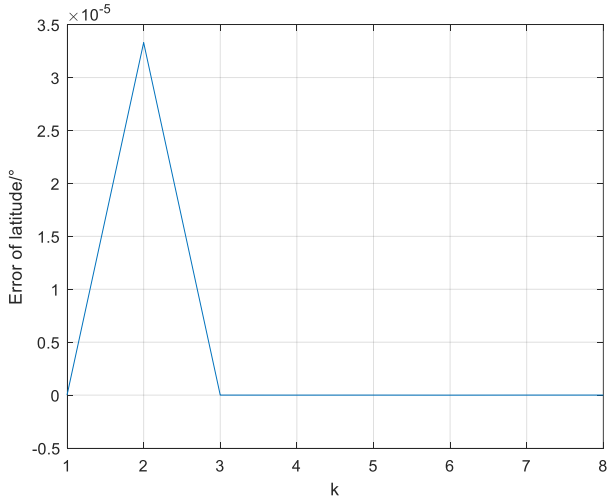

Figure 9. Estimation error of latitude of No.2 buoy in June 2020

Figures 5-9 show that the new algorithm can correctly predict the drift trajectories of buoys under long and short drift distances.

5.3 Performance Comparison of Different Algorithms

The standard deviation of latitude estimation error and longitude estimation error calculated by different algorithms for Meizhou Bay No. 11A buoy in 2020 is shown in Table 2.The parameter setting is the same as section 5.1.

Table 2. Estimation error of different algorithms

Methods	σ_{λ}/(°)	σ_{φ}/(°)
Neural Networks	5.34e-04	8.84e-05
CVNN	4.32e-04	7.66e-05
Improved CVNN	3.21e-04	6.36e-05

ISSN: 2414-1895 DOI: 10.6919/ICJE.202203_8(3).0011

The results show that the new algorithm can improve the prediction accuracy. It has a lower standard deviation of latitude prediction error and longitude prediction error.

6. Conclusion

In this paper, a buoy drift trajectory prediction based on an improved complex-valued neural network is designed, and a new algorithm is used to predict the buoy position drift trajectory with different reporting intervals. Experimental results and error analysis show that the algorithm outperforms other algorithms in trajectory prediction.

Future research will continue to improve this algorithm for better predictive power.

References

[1] GAN L X, XU C Y, ZHOU C H, et al. Early-warning method of buoy drift based on Kalman filtering and ISODATA[J]. Journal of Shanghai Maritime University, 2017, 38(4): 26-31.

[2] XU C Y. Research on Buoy Drift Warning and Cloud Management Platform[D]. Wuhan: Wuhan University of Technology,2018.

[3] CHENG X. Optimization study of anchor chain length of navigation buoys[J]. Journal of Waterway and Harbor, 2019, 40(2):226-230.

[4] ZHOU Y M, CHU X M, JIANG Z L, et al. Research on Drift Characteristics of Inland Navigation Buoy Based on Kalman Filtering and K-means++ Algorithm[J]. Journal of Wuhan University of Technology (Transportation Science & Engineering), 2019, 43(1): 81-85.

[5] CHEN Q L. Position Prediction of Light Buoy in Yangtze Estuary Deepwater Fairway[J]. Journal of Jimei University (Natural Science), 2020,25(4):272-278.

[6] ZHOU C H, ZHAO J N, GAN L X, et al. On the early warning method of the navigation buoy drift under the tidal current field[J]. Journal of Safety and Environment, 2021, 21(1): 217-223.

[7] WU Z Z, XIANG L, XIAO H, et al. Prediction the position of light buoy using multiplicative seasonal ARIMA model[J]. Electronic Measurement Technology, 2021,44(14),8-16.

[8] Chen, Q. Bin, H. Huang, Z. Event-based master–slave synchronization of complex-valued neural networks via pinning impulsive control. Neural Networks 2021, Doi: 10.1016/j.neunet.2021.10.025.

[9] Song, Q. Zhao, Z. Liu, Y. Alsaadi, F.E. Mean-square input-to-state stability for stochastic complex-valued neural networks with neutral delay. Neurocomputing 2021, Doi: 10.1016/j.neucom.2021.10.117.

[10] Huang, Y, Wu, F. Finite-time passivity and synchronization of coupled complex-valued memristive neural networks. Information Sciences 2021, 580: 775-800.

[11] Li, C. Liu, S. Wang, Z. Classifying interictal epileptiform activities in intracranial EEG using complex-valued convolutional neural network. International Journal of Psychophysiology 2021, 168: S104-S105.

[12] Song, X. Sun, X. Man, J. Song, S. Wu, Q. Synchronization of fractional-order spatiotemporal complex-valued neural networks in finite-time interval and its application. Journal of the Franklin Institute 2021, 358(16): 8207-8225.

[13] Aouiti, C. Bessifi, M. Sliding mode control for finite-time and fixed-time synchronization of delayed complex-valued recurrent neural networks with discontinuous activation functions and nonidentical parameters. European Journal of Control 2021, 59: 109-122.

[14] LIN Y H, PAN W R, XIAO Z, et al. Analysis of tidal current characteristics of the Xiamen Bay after the opening of Gaoji Seawall[J]. Transactions of Oceanology and Limnology, 2020, (6): 9-17.

[15] WANG M F, DENG B, JIANG C B, et al. Numerical study on propagation characteristics of ship waves in a restricted channel[J]. Journal of Water Resources & Water Engineering, 2020, 31(5): 157-163.

[16] ZHANG S Y, HUANG L H. Influence of ship wave on port[J]. Port & Waterway Engineering, 2018, 543 (6):159-162.